Efficient generation of human primordial germ cell-like cells from pluripotent stem cells in a methylcellulose-based 3D system at large scale

Xiaoman Wang [1, 2, 3], **Tingting Liao** [4], **Cong Wan** [2], **Xiaoyu Yang** [5], **Jiexiang Zhao** [2], **Rui Fu** [1], **Zhaokai Yao** [2], **Yaping Huang** [2], **Yujia Shi** [2], **Gang Chang** [6], **Yi Zheng** [2], **Fang Luo** [2], **Zhaoting Liu** [2], **Yu Wang** [Corresp., 1], **Xinliang Mao** [Corresp., 7], **Xiao-Yang Zhao** [2]

[1] State Key Laboratory of Stem Cell and Reproductive Biology, Institute of Zoology, Chinese Academy of Sciences, Beijing, China

[2] Department of Developmental Biology, School of Basic Medical Sciences, Southern Medical University, Guangzhou, Guangdong, China

[3] College of Life Sciences, University of the Chinese Academy of Sciences, Beijing, China

[4] Center for Reproductive Medicine, Changsha Hospital for Maternal and Child Health Care, Changsha, Hunan, China

[5] State Key Laboratory of Reproductive Medicine, Clinical Center of Reproductive Medicine, the First Affiliated Hospital of Nanjing Medical University, Nanjing, China

[6] Department of Biochemistry and Molecular Biology, Shenzhen University Health Science Center, Shenzhen, Guangdong, China

[7] School of Food Science and Engineering, South China University of Technology, Guangzhou, Guangdong, China

Corresponding Authors: Yu Wang, Xinliang Mao
Email address: wangyu@ioz.ac.cn, xlmao918@foxmail.com

Background. The mechanisms underlying human germ cell development and infertility remain largely unknown due to bioethical issues and the shortage of experimental materials. Therefore, an effective in vitro induction system of human primordial germ-like cells (hPGCLCs) from human pluripotent stem cells (hPSC) is in high demand. The current strategies used for the generation of hPGCLCs are not only costly but also difficult to perform at a large scale, thereby posing barriers to further research. In this study, we attempted to solve these problems by providing a new 3D culture system for hPGCLC differentiation.

Methods. The efficiency and relative yield of a methylcellulose (MC)-based 3D hPGCLC induction system were first compared with that of a conventional U96 system. Then, we examined the gene expression of germ cell marker genes and the key epigenetic modifications of the EpCAM-/INTEGRINα6-high cells from the 3D MC induction system and the U96 system via quantitative PCR and immunofluorescence. Finally, the reliability of the MC-based 3D hPGCLC induction system was evaluated via the generation of induced pluripotent stem cells (iPSCs) from the testicular cells of one patient with obstructive azoospermia (OA) and followed by the subsequent differentiation of iPSCs into the germ cell lineage.

Results. In the present study, we demonstrated that the 3D MC induction system combined with low-cell attachment plates facilitated the generation of hPGCLCs at a large scale. We found that the hPGCLCs generated via the MC system shared similar characteristics to that via the U96 system in terms of the gene expression profiles, germ cell-specific markers, epigenetic modification states and cellular states. In addition, hPGCLCs from iPSCs derived from one OA patient were generated with high efficiency via the the present 3D MC induction system.

Discussion. The in vitro induction of hPGCLCs from hESCs/hiPSCs has significant implications in exploring the underlying mechanisms of the origin and specification of hPGCs and the epigenetic programming of the human germ line as well as treating male infertility. Here, we developed a simple and efficient 3D induction system to generate hPGCLCs from hESCs/hiPSCs at a large scale, which facilitated the study of human germ cell development and stem cell-based reproductive medicine.

Efficient Generation of Human Primordial Germ Cell-Like Cells from Pluripotent Stem Cells in a Methylcellulose-Based 3D System at Large Scale

Xiaoman Wang[1,2,3,8], Tingting Liao[4,8], Cong Wan[2,9], Xiaoyu Yang[5,9], Jiexiang Zhao[2], Rui Fu[1], Zhaokai Yao[2], Yaping Huang[2], Yujia Shi[2], Gang Chang[7], Yi Zheng[2], Fang Luo[2], Zhaoting Liu[2], Yu Wang[1*], Xinliang Mao[6*], Xiao-Yang Zhao[2]

1. State Key Laboratory of Stem Cell and Reproductive Biology, Institute of Zoology, Chinese Academy of Sciences, Beijing, China
2. Department of Developmental Biology, School of Basic Medical Sciences, Southern Medical University, Guangzhou, Guangdong, China
3. College of Life Sciences, University of the Chinese Academy of Sciences, Beijing, China
4. Center for Reproductive Medicine, Changsha Hospital for Maternal and Child Health Care, Changsha, Hunan, China
5. State Key Laboratory of Reproductive Medicine, Clinical Center of Reproductive Medicine, the First Affiliated Hospital of Nanjing Medical University, Nanjing, China.
6. School of Food Science and Engineering, South China University of Technology, Guangzhou, Guangdong, China
7. Department of Biochemistry and Molecular Biology, Shenzhen University Health Science Center, Shenzhen, Guangdong, China
8. These authors contributed equally to this work.
9. There authors contributed equally to this work.

* Corresponding authors: Yu Wang (wangyu@ioz.ac.cn) and Xinliang Mao (xlmao918@foxmail.com).

Abstract

Background. The mechanisms underlying human germ cell development and infertility remain largely unknown due to bioethical issues and the shortage of experimental materials. Therefore, an effective in vitro induction system of human primordial germ-like cells (hPGCLCs) from human pluripotent stem cells (hPSC) is in high demand. The current strategies used for the generation of hPGCLCs are not only costly but also difficult to perform at a large scale, thereby posing barriers to further research. In this study, we attempted to solve these problems by providing a new 3D culture system for hPGCLC differentiation.

Methods. The efficiency and relative yield of a methylcellulose (MC)-based 3D hPGCLC induction system were first compared with that of a conventional U96 system. Then, we examined the gene expression of germ cell marker genes and the key epigenetic modifications of the EpCAM-/INTEGRINα6-high cells from the 3D MC induction system and the U96 system via quantitative PCR and immunofluorescence. Finally, the reliability of the MC-based 3D hPGCLC induction system was evaluated via the generation of induced pluripotent stem cells (iPSCs) from the testicular cells of one patient with obstructive azoospermia (OA) and followed by the subsequent differentiation of iPSCs into the germ cell lineage.

Results. In the present study, we demonstrated that the 3D MC induction system combined with low-cell attachment plates facilitated the generation of hPGCLCs at a large scale. We found that the hPGCLCs generated via the MC system shared similar characteristics to that via the U96 system in terms of the gene expression profiles, germ cell-specific markers, epigenetic modification states and cellular states. In addition, hPGCLCs from iPSCs derived from one OA patient were generated with high efficiency via the the present 3D MC induction system.

Discussion. The in vitro induction of hPGCLCs from hESCs/hiPSCs has significant implications

in exploring the underlying mechanisms of the origin and specification of hPGCs and the epigenetic programming of the human germ line as well as treating male infertility. Here, we developed a simple and efficient 3D induction system to generate hPGCLCs from hESCs/hiPSCs at a large scale, which facilitated the study of human germ cell development and stem cell-based reproductive medicine.

Introduction

In mammals, including humans, the earliest germ cells are primordial germ cells (PGCs), which are derived from early embryos. After a precise and complicated developmental process, PGCs finally differentiate into spermatozoa or oocytes. Germ cells are crucial for the transmission of genetic and epigenetic information to the next generation. Therefore, defects in the germline may lead to infertility and other severe diseases (Reik & Surani 2015). Although 10%–15% of couples are affected by infertility (Onat & Kizilkaya Beji 2012), the mechanisms underlying human germ cell development and infertility remain unknown mainly because of bioethical issues and the shortage of experimental materials, such as human embryos. Accordingly, an effective in vitro human germ cell induction system or disease model is in high demand and will not only facilitate an understanding of human germline development but also provide a platform for treating disorders arising from human germ cell defects (Nagamatsu & Hayashi 2017).

Recently, based on the knowledge of the in vivo mouse primordial germ cell (mPGC) specification, the in vitro mouse germ cell specification process was reconstituted from pluripotent stem cells (PSCs). The mouse PSCs were first induced into pre-gastrulation epiblast-like cells (EpiLCs) and then immediately differentiated into PGC-like cells (PGCLCs), which possessed the developmental capability for both spermatogenesis and oogenesis (Hayashi et al. 2012; Hayashi et al. 2011). As germ cell induction system can provide abundant experimental materials, it has been utilized as a powerful platform to investigate the regulatory networks and dynamic epigenetic modifications during mPGC specification (Aramaki et al. 2013a; Kurimoto et al. 2015; Murakami et al. 2016; Nakaki et al. 2013). Furthermore, based on this induction system, sperm-like cells or mature oocytes were generated in vitro through the PGCLCs derived from mouse ESCs/iPSCs (Hikabe et al. 2016; Zhou et al. 2016). And human PGCLCs (hPGCLCs) could also be induced from human PSCs (Irie et al. 2015; Sasaki et al. 2015). By employing hPGCLC induction systems, SOX17 and EOMES were identified to be critical factors for hPGCLC specification (Irie et al. 2015; Kojima et al. 2017), indicating that hPGCLC induction systems had great advantages in

exploring the mechanisms underling human germ cell development.

Although the in vitro hPGCLC induction systems recapitulated the development of hPGCs, some limitations still existed. During the induction of hPGCLCs, ultra-low cell attachment U-bottom 96-well plates or other similar plates were needed to enable the formation of embryoid bodies (EBs), followed by several days of suspension in induction medium. These steps are labour-intensive and dramatically limit the scale of hPGCLC production. On the other hand, many experiments are restricted for the insufficient production of hPGCLCs, including the proteome analysis of the dynamics of translation or the post-translation modification, which requires a large number of hPGCLCs. Therefore, an alternative solution was to employ a 3D culture system that allows more seeding cells to form embryonic bodies and thus saves both labour and medium. Collagen, methylcellulose (MC), and polymeric hydrogel biomaterials in combination with larger low-cell attachment plates were considered as the potential approaches to generate EBs efficiently (Jiang et al. 2015; Kothapalli & Kamm 2013; Otsuji et al. 2014). However, whether they can be used to induce PGCLCs remains unclear.

Here, we reported a modified system to robustly generate hPGCLCs from human pluripotent stem cells (hPSCs) at large scale, and the yielded hPGCLCs exhibited typical gene expression and epigenetic modification profiles similar to that of human PGCs. Our work allows for the establishment of a new large-scale hPGCLCs induction strategy and has implications for deciphering the mechanisms underlying human germline development.

Materials & Methods

Culture of hPSCs

The hESC/hiPSC lines (Fy-hES-3, Fy-hES-12, YiPS-1, and YiPS-2) were cultured in feeder-free medium (CA1001500; PSCeasy®, CELLAPY, Beijing, China) on Matrigel (354277; Corning, NY, USA). Cell media were changed daily. Cells were passaged every 5 to 7 days using EDTA

(CA3001500, PSCeasy).

Induction of iMeLCs and hPGLCs

The hESCs/hiPSCs on Matrigel were treated with TrypLE™ Express enzyme to enable their dissociation into single cells. The iMeLCs were induced by plating 2.0×10^5~3.0×10^5 cells per well of a human plasma fibronectin-coated 6-well plate in GK15 basal medium (GMEM with 15% KSR, 0.1mM NEAA, 1mM sodium pyruvate, 2mM L-glutamine, and 0.1mM 2-mercaptoethanol, all components purchased from Thermo Fisher (Waltham, MA USA)containing 50 ng/ml of ACTA (R&D Systems, Minneapolis, MN USA), 3μM of CHIR99021 (TOCRIS, Bristol, UK) and 10μM of a ROCK inhibitor (Cat.1254/10, R&D Systems).

The hPGCLCs were induced via two methods: one was the conventional method in the ultra-low attachment surface round bottom 96-well plate (Cat. No.7007, Corning), and the other was the new method, which added MC in the medium in the 6-well low-cell-binding plate (Cat. No.150239, Thermo Fisher). With the first method, hPGCLCs were induced by planting 3.0×10^3/100μl iMeLCs into a well of ultra-low attachment surface round bottom 96-well plate in GK15 basal medium with 500 ng/ml of BMP4 (Peprotech, Rocky Hill, NJ USA), 100 ng/ml of LIF (Peprotech), 100 ng/ml of SCF (R&D Systems), 50 ng/ml of EGF (R&D Systems), and 10μM of the ROCK inhibitor (Y27632, R&D Systems), which was hPGCLC medium. One day later, the EBs formed, and the old 50 μl medium was replaced every two days. With the 3D MC based induction system, 2 ml of the 1:7 mixture of MC and hPGCLCs medium was added into one well of 6-well low-cell-binding plate, and then, 5×10^3~10×10^3 total iMeLCs in 1 μl cell suspension were seeded in 0.35% MC medium with 50-60 replicates. One well of 6-well plate was suitable for plating 4.0×10^5-6.0×10^5 iMeLCs. After one day, the EBs formed. On the next day, the dead cells and the cell debris were eliminated after centrifugations at 600 rpm for 1 min followed by re-suspending the EBs with 2 ml fresh MC medium and plating into the well. Half of the medium was replaced every two days.

Fluorescence-activated cell sorting

Day 4-8 EBs were washed in PBS and dissociated with 0.25% trypsin/ EDTA for 8-15 min at

37°C. Dissociated cells were resuspended in FACS solution consisted of 2% (v/v) fetal bovine serum (FBS) in PBS. Samples were stained with APC-conjugated anti-human CD326 (EpCAM) and BV421-conjugated anti-human/mouse CD49f (INTEGRINα6) for 15 min at 4°C. FACS analysis was performed using the FACS Calibur system (Becton Dickinson, Franklin Lakes, NJ USA).

Quantitative PCR

Total RNA was extracted from cells using Trizol (Life Technologies, Carlsbad, CA USA) according to the manufacturer's instructions. Synthesis of cDNA for Q-PCR using less than 2 μg of purified total RNA was performed as in the technical manual using GoScript™ Reverse Transcription System (Promega, Madison, WI USA), and the first-strand cDNAs were used for quantitative PCR analysis with 2×RealStar Green Fast Mixture (GenStar, Beijing, China) using LightCycler96™ system (Roche, Basel, Switzerland). The gene expression levels were examined by calculating ΔCt (in log2 scale) normalized to the average ΔCt values of ARBP. Error bars are mean ± SD from two or three independent experiments. The primer sequences are listed in Table S1.

Immunofluorescence

Day 4 EBs induced from hESCs/hiPSCs were fixed in 4% paraformaldehyde in PBS for 1 h, then washed twice in PBS and incubated with 30% sucrose for 1 h at 4°C.The samples then were embedded in OCT embedding matrix and stored at -80°C. Subsequently, samples were sliced into 7-μm cryosections by a cryostat (Leica, Heidelberger, Germany). Before immunofluorescence, slides with cryosections were air dried at room temperature for at least 15 min. Next, the slides were incubated in blocking solution (2% bovineserum albumin, 1× PBS) for 1 h at room temperature followed by incubation with primary antibodies in blocking solution overnight at 4°C. After washing with PBS for three times, the slides were incubated with secondary antibodies in blocking solution for 1 h at room temperature, washed three times with PBS again, and then incubated with 10 μg/mL of Hoechst for 15 min at room temperature. The slides were then washed twice with PBS before being mounted in anti-fading Mounting Medium (Solarbio, Beijing, China)

for confocal laser scanning microscope analysis (Carl Zeiss LSM 880, AxioObserver). For 5hmC staining, slides were subjected to heat-induced epitope retrieval in antigen retrieval buffers (ZSGB-BIO, Beijing, China) by a microwave oven. After retrieval, slides were cooled to room temperature and washed in PBS for three times. For H3K9me2 and H3K27me3 staining, EpCAM/INTEGRINα6-high cells at day 4 of induction from Fy-hES-3 or YiPS were mixed with Fy-hES-3 or YiPS, respectively, at a ratio of 1:1, spread onto poly-L-lysine-coated glass slides (CITOGLAS, Jiangsu, China) by Cytospin4 (Thermo Fisher) and fixed with 4% paraformaldehyde in PBS. The slides were washed with PBS for three times, incubated in blocking solution for 1 h and incubated with primary antibodies in blocking solution overnight. Primary antibodies were listed as follows: Mouse anti-Oct-3/4 (1:400, sc-5279; Santa Cruz, Dallas, Texas, USA), Goat anti-Oct-3/4 (1:400, sc-5279; Santa Cruz, Dallas, Texas, USA), Rabbit anti-Sox2 (1:500, Ab97959,Abcam, Cambridge, UK), Goat anti-Nanog (1:400, AF1997, R&D Systems), Mouse anti-SSEA4 (1:500, Abcam), Goat anti-Sox17 (1:200, AF1924, R&D Systems,), Rabbit anti-AP-2γ (1:400, sc-8977; Santa Cruz, Dallas, Texas, USA), Rat anti-Blimp1(1:200, 14-5963-82, Thermo Fisher), Mouse anti-H3K9me2 (1:500, Ab1220, Abcam), Mouse anti-H3K27me3 (1:500, Ab6002, Abcam), Anti-5hmc (1:400, 39769; Active Motif, Carlsbad, CA USA). Images were obtained with ZEISS LSM880 confocal microscope.

Image analysis

Analyses and quantifications were performed with ImageJ Software (1.51k). To quantify the fluorescence intensity of H3K9me2 and H3K27me3 in the confocal images of slides spread by Cytospin4, a custom workflow was designed in the ImageJ User Guide. Briefly, each individual nucleus was selected based on its Hoechst signal. Nuclei that overlapped with TFAP2C signals were defined as hPGCLCs, while the rest were defined as hESCs/hiPSCs. The fluorescence intensities for the H3K9me2 and H3K27me3 of interest were then measured in the two populations of nuclei, and the distributions were plotted in scatter plots. The fluorescence intensities of 5hmC of EBs sections were measured based on the above workflow as well.

Inducing integration-free human induced pluripotent stem cells

196 The human testicular cells were obtained from an obstructive azoospermia patient. During 2 or 3
197 culture passages, cells were transfected with an episomal vector encoding 6 factors (Oct4, Sox2,
198 Nanog, Lin28, Klf4, and L-MyC). After inducting in N2B27 medium for 2 weeks, the samples
199 showed distinct small colonies were picked and expanded into PSCeasy Medium.

200 **Karyotyping analyses and alkaline phosphatase staining**

201 hiPSCs were incubated with culture medium containing 100 ng/mL of colchicine (Sigma-Aldrich,
202 St. Louis, MO USA) for 8 h. Dissociated cells were subjected to hypotonic treatment with 1%
203 sodium citrate for 30 min at room temperature, followed by fixation in Carnoy's solution (3:1
204 mixture of methanol and acetic acid) and dropped onto glass slides placed on a sheet of water-
205 soaked paper. Chromosomes were visualized by Giemsa staining. Images were captured on a Leica
206 DM 6000 B microscope. Alkaline phosphatase staining was performed using the Leukocyte
207 Alkaline Phosphatase kit (Sigma-Aldrich).

208 **In vitro differentiation**

209 For EB formation, YiPS cells were harvested by treating with collagenase IV. Cell clumps were
210 transferred to a well of 12-well low-cell-binding plate in DMEM/F12 Medium containing 20%
211 knockout serum replacement (KSR, Invitrogen), 2 mM L-glutamine, 0.1 mM 2-mercaptoethanol
212 (Invitrogen), 0.1 mM NEAA, and 0.5% penicillin and streptomycin. The medium was changed
213 every other day. After 8 days' floating culture, EBs were transferred to Matrigel-coated plates and
214 cultured in the same medium for another 8~12 days. The RNA derived from plated EBs cells was
215 extracted for RT-PCR.

216 **Teratoma formation**

217 hiPSCs were harvested by treating with collagenase IV. About 2×10^6 cells were suspended by
218 100 µl DF12 mixed with 50 µl Matrigel and injected subcutaneously to dorsal flank of a SCID
219 mouse. 6~9 weeks after injection, tumors were dissected, weighed, and fixed with Carnoys
220 fixative. Paraffin-embedded tissues were sliced and stained with hematoxylin and eosin. Sections
221 were examined for the presence of tissue representatives of all three germ layers.

222 **Statistical analysis**

For statistical analyses, the data of the fluorescence intensity of H3K9me2, H3K27me3 and 5hmC were analyzed by Mann Whitney test and other data were analysed by t-test. Quantitative results were expressed as the mean ± standard deviation (SD). Statistical significance was reached when $P< 0.05$. $*P < 0.05$, $**P < 0.01$, $***P < 0.001$, $****P < 0.0001$.

Results

3D MC induction system facilitates hPGCLC differentiation

MC is widely used in 3D culture for cell suspension and it could significantly increase the yield of target cells and generate more mature cells or tissue types (Jiang et al. 2015; Kothapalli & Kamm 2013; Lee & Park 2016; Otsuji et al. 2014). Therefore, we aimed to test the efficiency of a MC-based 3D hPGCLC induction system. Two male hESCs cell lines (Fy-hES-3 and Fy-hES-12, gifts from the Professor Yong Fan) were used to induce hPGCLCs in the modified system (Fig. 1A). Both cell lines shared similar celluar characteristics, and Fy-hES-3 was shown as a representative result. The hESCs were efficiently differentiated into incipient mesoderm-like cells (iMeLCs), in which classical pluripotency markers including OCT4, NANOG and SOX2 were expressed (Fig. S1A and S1B). According to the previous report (Jiang et al. 2015), we initially adopted 0.35% MC in PGCLC medium and found that it could effectively facilitate the iMeLCs in generating solid EBs, from which a high ratio of EpCAM-/INTEGRINα6-high cells could be obtained. In contrast, there were only adherent cells in the bottom of flat plate without MC and much lower percentage of EpCAM/INTEGRINα6-high cells was observed (Fig. 1B; Figs. S1C and S1D). Compared to the original protocol, in which an ultra-low cell attachment U-bottom 96-well was used for the formation of EBs in hPGCLC induction (Sasaki et al. 2015), the hPGCLC induction efficiency in the 0.35% MC system was elevated in day 4 EBs (Fig. 1C). The effect of different concentrations of MC on inducing hPGCLCs was also tested, respectively. We found that 0.1% MC resulted in the decreased and instable differentiation efficiency compared to that of 0.35% MC, whereas the outcome of using 0.7% MC was similar to that of 0.35% MC (Figs. 1C and 1D). A little bit higher ratio of EpCAM-/ INTEGRINα6-high cells could be obtained from day 4 EBs

to day 8 EBs in the MC group than the U96 group (Fig. 1E). However, there was no obvious difference in the ratio of EpCAM-/INTEGRIN α6-high cells at day 4 EBs via U96 method and U96 with different concentrations of MC method (Fig. S1E). In addition, when one microliter cell suspensions containing 5×10^3~1×10^4 iMeLCs were used via 0.35% MC method, the proper size of EBs and a little bit higher ratio of hPGCLCs were obtained. In contrast, when more than 1.5×10^4 iMeLCs were seeded, EBs with bigger diameter were formed and decreased efficiency of hPGCLCs induction were observed (Fig. 1F). Notably, the increase of induction efficiency was more obvious in the day 4 but decreased in day 6 (Fig. 1G). In general, the numbers of hPGCLCs for one well of a 6-well plate via MC system were nearly twice the numbers of hPGCLCs generated from a U96 plate partially owing to more seeding cells in MC group without damaging the efficiency (Fig. S1F). Furthermore, the induction yield of hPGCLCs from the MC group was approximately 8-10 times higher than that of the U96 group at the same consumption level of hPGCLC medium (Fig. 1H; Table 1). Therefore, the 3D MC induction system combined with low cell attachment plates that had larger volume, such as 6-well plates, facilitated the generation of hPGCLCs at large scale.

The EpCAM-/INTEGRINα6-high cells from MC induction system exhibited the transcriptional characteristics of hPGCLCs

Next, we examined the gene expression profiling of the EpCAM-/INTEGRINα6-high cells from the 3D MC induction system. Q-PCR analysis showed that the gene expression profiling of day 4 EpCAM-/INTEGRINα6-high cells from the MC group were highly similar to that from the U96 group. Compared to iMeLCs, day 4 EpCAM-/INTEGRINα6-high cells showed slightly elevated expressions of *OCT4* and *NANOG*, whereas *SOX2* exhibited a greatly decreased expression pattern. With respect to the genes related to naïve pluripotency, *ZFP42* and *PRDM14* were downregulated, while *KLF4* and *ESRRB* were highly upregulated. hPGCLCs specification genes, including *SOX17, BLIMP1, NANOS3* and *TFAP2C*, were highly elevated in EpCAM-/INTEGRINα6-high cells, whereas *STELLA* was slightly upregulated. In addition, a later PGC marker gene *DAZL* showed downregulated expression. For endoderm or mesoderm marker genes,

277 *GATA4*, *T* and *EVX1* showed obvious elevated expression in EpCAM-/INTEGRINα6-high cells.
278 Activated in iMeLCs, *NODAL* was drastically downregulated. On the other hand, *DNMT3A* and
279 *DNMT3B*, *de novo* DNA methyltransferases associated with DNA methylation in mammals, were
280 downregulated markedly (Fig. 2A). Thus, the gene expression patterns of PGCLCs from both
281 groups were similar, which was consistent with the previous study (Irie et al. 2015; Sasaki et al.
282 2015). Immunofluorescence analyses confirmed the high ratio of SOX17-positive cells in EBs and
283 the OCT4-positive cells were also BLIMP1 and TFAP2C-positive cells (Fig. 2B). In addition, the
284 ratio of SOX17-positive cells of day 4 EBs of 3D MC group was significantly higher than that of
285 U96 group, which was consistent with the EpCAM/INTEGRINα6 FACS results (Fig.1G; Fig. 2C).
286 In summary, these findings proved that EpCAM-/INTEGRINα6-high cells from both groups
287 shared a high similarity in terms of gene expression.

288 **hPGCLCs from 3D MC group exhibited key epigenetic properties and cellular**
289 **characteristics similar to that from U96 group**

290 To further confirm the identity of hPGCLCs, the epigenetic properties of hPGCLCs induced from
291 the 3D MC group and U96 group were then evaluated. Compare to hESCs, the
292 immunofluorescence analysis of day 4 hPGCLCs marked by TFAP2C was shown to have reduced
293 H3K9me2 expression level and elevated H3K27me3 expression level (Fig. 3A). In addition,
294 hPGCLCs exhibited an elevated expression level of 5hmC compare to that of hESCs (Fig. 3B).
295 We next compared cellular viability, proliferation, apoptosis and cell cycle of EBs between the
296 U96 group and 3D MC group. The cellular viability of EBs could be estimated by the percentages
297 of P1 gates (FSC/SSC) in FACS plot (Sasaki et al. 2015). FACS analysis of day 4 EBs showed
298 that the percentages of P1 gates had no difference (73.0% *vs* 75.5%) in two groups, and the ratio
299 of P1 gates in day 6 EBs maintained the same pattern (Fig. 3C). The cell cycle also had no
300 difference between both groups (Fig. 3D). Moreover, 7-AAD and Annexin V could be used to
301 distinguish viable, early apoptotic, and late apoptotic/dead cells in flow cytometry (Nadine et al.
302 2012). We found that the day 4 EBs from MC group revealed a decreased ratio of apoptosis,
303 including early- and late-stage apoptosis via FACS analysis with 7-AAD and Annexin V (Fig. 3E).

Antigen Ki-67 is a nuclear protein that is associated with and may be necessary for cellular proliferation. Immunofluorescence analyses exhibited that the ki-67 positive cells accounted for similar percentages (18%) of germ cells, marked by TFAP2C, in EBs for both U96 and MC groups, suggesting that hPGCLCs in EBs under two conditions had similar proliferation capacity (Fig. 3F). Thus, EBs from the MC group showed a high quality by exhibiting a decreased percentage of apoptosis. In summary, hPGCLCs from 3D MC method showed similar epigenetic properties and cellular characteristics with that from U96 method.

hPGCLCs derived from hiPSCs were generated in 3D MC induction system

To test the utility of the MC-based 3D hPGCLC induction, iPSCs were generated and further induced to germ cells lineage in vitro. Two hiPSC lines (named YiPS-1, YiPS-2) were induced from somatic cells of testes (donated by one patient with obstructive azoospermia) by the ectopic expression of an episomal vector containing six factors (Oct4, Sox2, Nanog, Lin28, Klf4, and L-MyC) (Fig. 4A; Fig. S2A). hiPSC clones were positive for alkaline phosphatase (AP) staining (Fig. S2B). PCR analysis of oriP and EBNA-1 in two hiPSC lines (YiPS-1 and YiPS-2) revealed the episomal vector was absent in the yielded hiPSCs (Fig. S2C). Since both hiPSC lines shared similar results, Yips-1 was shown as a representative for later experiments. Karyotype analysis of YiPS-1 showed 46/XY that excluded the chromosome abnormality (Fig. S2D). Q-PCR results showed YiPS cells expressed typical pluripotent marker genes, such as *OCT4*, *SOX2*, *NANOG*, *REX1* and *DPPA3* (developmental pluripotency-associated 3) at levels similar to that of hESC H9 (Fig. S2E). Immunostaining results further confirmed that YiPS cells expressed key human pluripotent markers, including OCT4, SOX2 and SSEA4 (Fig. S2F). To determine the differentiation ability of YiPS cells in vitro, iPSCs were differentiated into EBs. YiPS cells formed EBs in suspension culture for 8 days in low-cell-binding plate (Fig. S3A). Then the EBs were transferred to Matrigel-coated plates for 8 days and attached cells on Matrigel showed epithelial morphologies (Fig. S3B) or other types of morphologies (data not shown). RT-PCR analysis showed that these differentiated cells on Matrigel expressed *AFP* (Alpha-fetoprotein, endoderm), *SOX17* (SRY-box containing gene 17, endoderm), *MSX1* (Msh homeobox 1, mesoderm) and *MAP2* (Microtubule-associated

protein 2, ectoderm) (Fig. S3C). Teratomas were observed after YiPS cells were subcutaneously injected into severe combined immunodeficiency (SCID) mice at week 6. HE (haematoxylin and eosin-stain) analysis showed that the teratomas contained all three embryonic germ layers including the ectoderm, mesoderm and endoderm (Fig. S3D).

Then, the YiPS-1 cells were induced to hPGCLCs with a 3D MC induction protocol. The iMeLCs showed a similar morphology to that of hESCs (Fy-hES-3) and expressed pluripotency markers, such as OCT4, NANOG and SOX2 (Fig. S4A and S4B). The hiPSCs efficiently differentiated into hPGCLCs, both in the U96 group and 3D MC group (Fig. 4B). Q-PCR analysis showed that hPGCLCs derived from two groups had a similar gene expression pattern, which was consistent with that of Fy-hES-3. Compared to iMeLCs, hPGCLCs had elevated expression levels of *OCT4*, *NANOG* and *KLF4*, reduced expression of *PRDM14* and *SOX2*, and upregulated expression of genes specifically involved in hPGCLC specification, such as *SOX17*, *BLIMP1*, *TFAP2C* and *NANOS3* (Fig. 4C). Immunofluorescence analyses further confirmed the expression of OCT4, TFAP2C and SOX17 in EBs (Fig. 4D). In contrast to hiPSCs, hPGCLCs exhibited lower level of H3K9me2 and higher level of H3K27me3, which were consistent with results from hPGCLCs of Fy-hES-3 (Fig. 3A; Fig. 4E). The TFAP2C-positive cells showed a high level of 5hmC compared with that of TFAP2C negative cells (Fig. 4F). The EBs derived from YiPS-1 cells in MC group had similar cell cycle and decreased rate of apoptosis compared to EBs in U96 group (Fig. S4C and S4D). The relative induction yield of hPGCLCs from YiPS-1 cells in the MC condition was about 8 times higher than that of the U96 group (Fig. S4E). In summary, about 20% EpCAM-/INTEGRINα6-high cells were induced from YiPS-1 cells via 0.35% MC method and these cells shared the characteristics of hPGCLCs including the gene expression pattern and epigenetic modification.

Discussion

The success in obtaining hPGCLCs from hPSCs provides us with a model to recapitulate the processes of hPGCLC specification and maintenance. However, unlike mPGCLCs, which can

further form functional spermatozoa or germinal vesicle-stage oocytes in vivo or in vitro, hPGCLCs do not show this potential due to several challenges, such as the potential of tumour formation risk after in vivo transplantation or the limitation of materials such as somatic cells from human gonads for in vitro gamete differentiation. On the other hand, the mechanisms underlying human PGC specification were largely unknown. Although differential gene expression analysis, especially transcriptome, has provided important clues to identify the essential transcription factors during hPGCLC induction such as SOX17 and EOMES (Irie et al. 2015; Kojima et al. 2017), it is still far from figuring out the detailed mechanisms underlying germ cells specification. Further omic studies should be performed such as proteomics and ATAC-seq, which required a large number of hPGCLCs (Gao et al. 2017; Guo et al. 2017). Therefore, the efficient generation of hPGCLCs at large scale would facilitate the investigations of in vitro gamete differentiation from hPSCs and the regulatory mechanisms of hPGC/hPGCLC specification.

Although ultra-low cell attachment U-bottom 96-well plates or other similar plates have been wildely used to enable the generation of EBs during the induction of hPGCLCs, this strategy restricts the seeding density of cells (3×10^5~4×10^5 cells for an U96 plate) and increase the medium consumption. The process is therefore costly and labour intensive, which are not compatible with producing hPGCLCs at large scale. To generate hPGCLCs via an economic and scalable way, we employed MC to aggregate dissociated iMeLCs to produce floating EBs, in which hPGCLCs were induced effectively. Compared with the U96 method, we obtained a higher relative yields ratio of hPGCLCs via MC-based strategyGene expression levels including key germ cell markers and epigenetic properties of hPGCLCs from the MC method are similar to hPGCLCs from the U96 system. In addition, the aggregates from the MC method showed similar cell viability states, cell cycle and proliferation capacity and decreased rate of apoptosis compared to the aggregates from the U96 method. On the other hand, the MC method could be used to the induction of hPGCLCs from iPSCs, implying the potential clinical application value.. It should be noted that our MC method depends on iMeLCs from a 2D condition, and it can be anticipated that a further elevated yield of hPGCLCs could be achieved after optimizing the culture system by performing the whole

induction process from hPSCs to hPGCLCs in a 3D condition.

Conclusions

Here, we developed a simple and efficient 3D induction system to generate hPGCLCs from human pluripotent stem cells at large scale. These hPGCLCs showed similar critical characteristics of those from the conventional U96 protocol, including gene expression, germ cell markers, and epigenetic properties. Furthermore, we generated iPSCs and then differentiated them into hPGCLCs efficiently, which indicated both human ESCs and iPSCs could efficiently differentiate into hPGCLCs at large scale by our new 3D system.

Acknowledgements

We are grateful to Dr. Yong Fan for providing us with the human ESC lines Fy-hES-3 and Fy-hES-12. We thank all members of the Group for Stem Cell and Regenerative Medicine for discussion and help. We also appreciate help from Beckman Coulter Inc. for the FACS sorting.

References

Aramaki S, Hayashi K, Kurimoto K, Ohta H, Yabuta Y, Iwanari H, Mochizuki Y, Hamakubo T, Kato Y, Shirahige K, and Saitou M. 2013b. A mesodermal factor, T, specifies mouse germ cell fate by directly activating germline determinants. *Dev Cell* 27:516-529. 10.1016/j.devcel.2013.11.001

Chen D, Liu W, Lukianchikov A, Hancock G, Zimmerman J, Lowe M, Kim R, Galic Z, Irie N, Surani MA, Jacobsen SE, and Clark AT. 2017. Germline competency of human embryonic stem cells depends on EOMESODERMIN. *Biol Reprod*. 10.1093/biolre/iox138

Gao Y, Liu X, Tang B, Li C, Kou Z, Li L, Liu W, Wu Y, Kou X, Li J, Zhao Y, Yin J, Wang H, Chen S, Liao L, and Gao S. 2017. Protein Expression Landscape of Mouse Embryos during Pre-implantation Development. *Cell Rep* 21:3957-3969. 10.1016/j.celrep.2017.11.111

Guo J, Grow EJ, Yi C, Mlcochova H, Maher GJ, Lindskog C, Murphy PJ, Wike CL, Carrell DT, Goriely A, Hotaling JM, and Cairns BR. 2017. Chromatin and Single-Cell RNA-Seq Profiling Reveal Dynamic Signaling and Metabolic Transitions during Human Spermatogonial Stem Cell Development. *Cell Stem Cell* 21:533-546 e536. 10.1016/j.stem.2017.09.003

Hayashi K, Ogushi S, Kurimoto K, Shimamoto S, Ohta H, and Saitou M. 2012. Offspring from oocytes derived from in vitro primordial germ cell-like cells in mice. *Science* 338:971-975. 10.1126/science.1226889

Hayashi K, Ohta H, Kurimoto K, Aramaki S, and Saitou M. 2011. Reconstitution of the mouse germ cell specification

pathway in culture by pluripotent stem cells. *Cell* 146:519-532. 10.1016/j.cell.2011.06.052

Hikabe O, Hamazaki N, Nagamatsu G, Obata Y, Hirao Y, Hamada N, Shimamoto S, Imamura T, Nakashima K, Saitou M, and Hayashi K. 2016. Reconstitution in vitro of the entire cycle of the mouse female germ line. *Nature* 539:299-303. 10.1038/nature20104

Irie N, Weinberger L, Tang WW, Kobayashi T, Viukov S, Manor YS, Dietmann S, Hanna JH, and Surani MA. 2015. SOX17 is a critical specifier of human primordial germ cell fate. *Cell* 160:253-268. 10.1016/j.cell.2014.12.013

Jiang B, Xiang Z, Ai Z, Wang H, Li Y, Ji W, and Li T. 2015. Generation of cardiac spheres from primate pluripotent stem cells in a small molecule-based 3D system. *Biomaterials* 65:103-114. 10.1016/j.biomaterials.2015.06.024

Kojima Y, Sasaki K, Yokobayashi S, Sakai Y, Nakamura T, Yabuta Y, Nakaki F, Nagaoka S, Woltjen K, Hotta A, Yamamoto T, and Saitou M. 2017. Evolutionarily Distinctive Transcriptional and Signaling Programs Drive Human Germ Cell Lineage Specification from Pluripotent Stem Cells. *Cell Stem Cell* 21:517-532 e515. 10.1016/j.stem.2017.09.005

Kothapalli CR, and Kamm RD. 2013. 3D matrix microenvironment for targeted differentiation of embryonic stem cells into neural and glial lineages. *Biomaterials* 34:5995-6007. 10.1016/j.biomaterials.2013.04.042

Kurimoto K, Yabuta Y, Hayashi K, Ohta H, Kiyonari H, Mitani T, Moritoki Y, Kohri K, Kimura H, Yamamoto T, Katou Y, Shirahige K, and Saitou M. 2015. Quantitative Dynamics of Chromatin Remodeling during Germ Cell Specification from Mouse Embryonic Stem Cells. *Cell Stem Cell* 16:517-532. 10.1016/j.stem.2015.03.002

Lee W, and Park J. 2016. 3D patterned stem cell differentiation using thermo-responsive methylcellulose hydrogel molds. *Sci Rep* 6:29408. 10.1038/srep29408

Murakami K, Gunesdogan U, Zylicz JJ, Tang WWC, Sengupta R, Kobayashi T, Kim S, Butler R, Dietmann S, and Surani MA. 2016. NANOG alone induces germ cells in primed epiblast in vitro by activation of enhancers. *Nature* 529:403-407. 10.1038/nature16480

Nagamatsu G, and Hayashi K. 2017. Stem cells, in vitro gametogenesis and male fertility. *Reproduction* 154:F79-F91. 10.1530/REP-17-0510

Nakaki F, Hayashi K, Ohta H, Kurimoto K, Yabuta Y, and Saitou M. 2013. Induction of mouse germ-cell fate by transcription factors in vitro. *Nature* 501:222-226. 10.1038/nature12417

Onat G, and Kizilkaya Beji N. 2012. Effects of infertility on gender differences in marital relationship and quality of life: a case-control study of Turkish couples. *Eur J Obstet Gynecol Reprod Biol* 165:243-248. 10.1016/j.ejogrb.2012.07.033

Otsuji TG, Bin J, Yoshimura A, Tomura M, Tateyama D, Minami I, Yoshikawa Y, Aiba K, Heuser JE, Nishino T, Hasegawa K, and Nakatsuji N. 2014. A 3D Sphere Culture System Containing Functional Polymers for Large-Scale Human Pluripotent Stem Cell Production. *Stem Cell Reports* 2:746. 10.1016/j.stemcr.2014.04.013

Reik W, and Surani MA. 2015. Germline and Pluripotent Stem Cells. *Cold Spring Harb Perspect Biol* 7. 10.1101/cshperspect.a019422

Sasaki K, Yokobayashi S, Nakamura T, Okamoto I, Yabuta Y, Kurimoto K, Ohta H, Moritoki Y, Iwatani C, Tsuchiya H, Nakamura S, Sekiguchi K, Sakuma T, Yamamoto T, Mori T, Woltjen K, Nakagawa M, Yamamoto T, Takahashi K, Yamanaka S, and Saitou M. 2015. Robust In Vitro Induction of Human Germ Cell Fate from

Pluripotent Stem Cells. *Cell Stem Cell* 17:178-194. 10.1016/j.stem.2015.06.014

Zhou Q, Wang M, Yuan Y, Wang X, Fu R, Wan H, Xie M, Liu M, Guo X, Zheng Y, Feng G, Shi Q, Zhao XY, Sha J, and Zhou Q. 2016. Complete Meiosis from Embryonic Stem Cell-Derived Germ Cells In Vitro. *Cell Stem Cell* 18:330-340. 10.1016/j.stem.2016.01.017

Figure 1

Evaluation of MC and ultra-low cell attachment U96 culture for hPGCLC differentiation.

(A) Flow chart of hPGCLC induction system based on 0.35% MC or U96 plate. (B) Bright field image of hPGCLCs floating aggregates cultured in hPGCLC medium containing 0.35% MC at day 4. Scale bar, 500 μm. (C) FACS analysis of the ratio of EpCAM-/INTEGRINα6-high cells of the D4 EBs of Fy-hES-3 under different MC concentrations. (D) The effect of MC concentrations on the ratio of EpCAM-/INTEGRINα6-high cells of the D4 EBs of Fy-hES-3. (E) FACS analysis of the proportion of EpCAM-/INTEGRINα6-high cells during the hPGCLC induction (from day 4 to day 8) of Fy-hES-3. (F) The effect of different numbers of iMeLCs per microliter seeding suspension medium on the proportion of EpCAM-/INTEGRINα6-high cells of day 4 EBs from Fy-hES-12 . One microliter of cell suspensions containing 5×10^3~2×10^4 iMeLCs were pipetted in hPGCLC medium containing 0.35% MC. (G) Differentiation efficiencies were compared between U96 method and 0.35% MC method from day 4 to day 6. *$P < 0.05$. (H) The relative yields of hPGCLCs at day 4 via 0.35% MC method and U96 method, respectively. Left, the relative number of hPGCLCs from one U96 plate or one well of the low-attachment 6-well plate; right, the relative number of hPGCLCs for 1 ml medium consumption via U96 method and 0.35% MC method. Both of them were calculated at day 4 during hPGCLC induction, and the number of hPGCLCs from U96 plate was set to 1 for reference. *$P < 0.05$. Error bars, SD (n = 3 measurements).

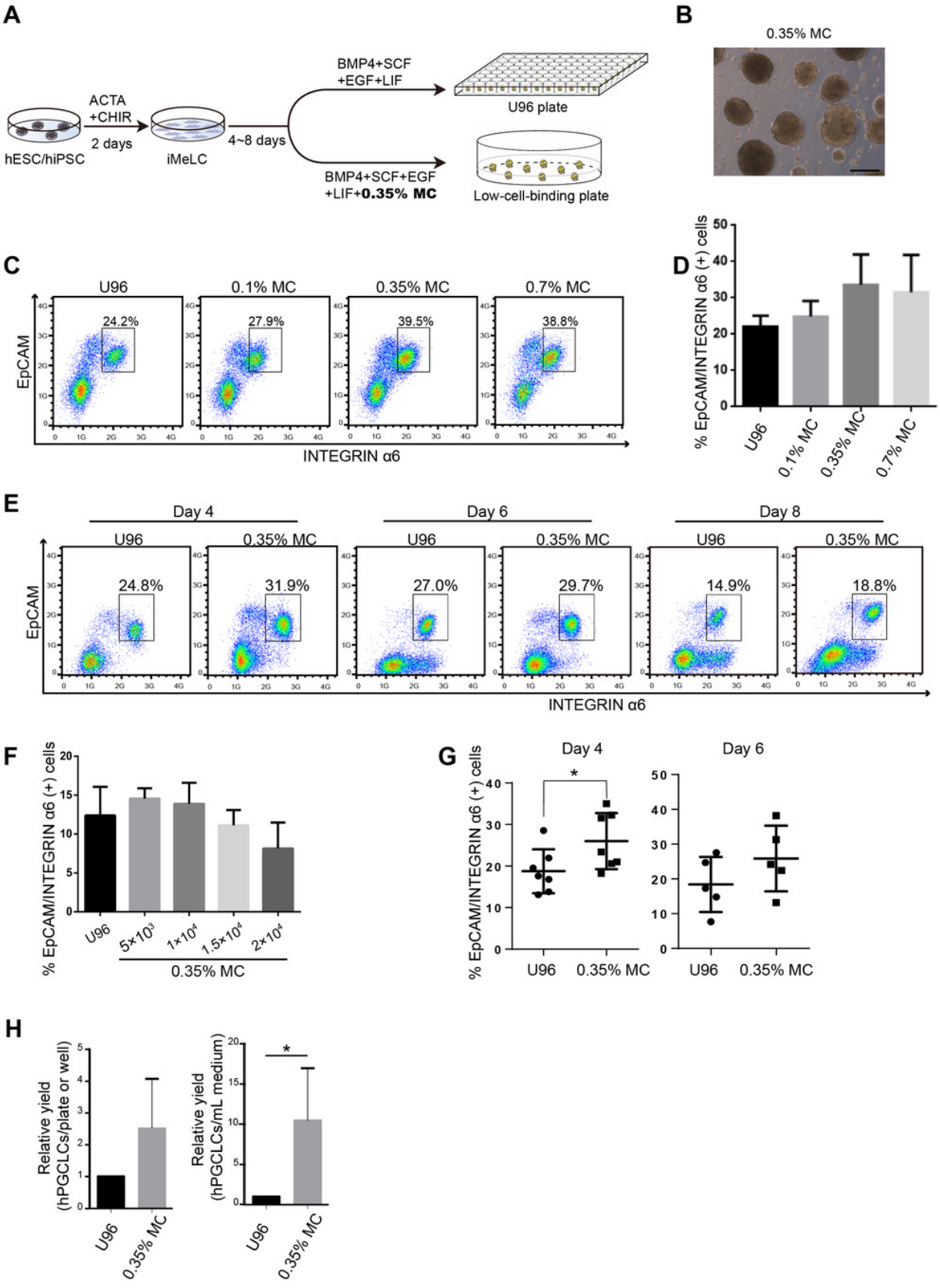
A
hESC/hiPSC
ACTA
+CHIR
2 days
iMeLC
4~8 days
BMP4+SCF
+EGF+LIF
U96 plate
BMP4+SCF+EGF
+LIF+0.35% MC
Low-cell-binding plate
B
0.35% MC
C
U96
0.1% MC
0.35% MC
0.7% MC
24.2%
27.9%
39.5%
38.8%
EpCAM
INTEGRIN α6
D
% EpCAM/INTEGRIN α6 (+) cells
U96
0.1% MC
0.35% MC
0.7% MC
E
Day 4
Day 6
Day 8
U96
0.35% MC
24.8%
31.9%
27.0%
29.7%
14.9%
18.8%
EpCAM
INTEGRIN α6
F
% EpCAM/INTEGRIN α6 (+) cells
U96
5×10³
1×10⁴
1.5×10⁴
2×10⁴
0.35% MC
G
Day 4
Day 6
*
% EpCAM/INTEGRIN α6 (+) cells
U96
0.35% MC
U96
0.35% MC
H
Relative yield
(hPGCLCs/plate or well)
Relative yield
(hPGCLCs/mL medium)
*
U96
0.35% MC
U96
0.35% MC

Figure 2

Similar gene expression profile and germ cell-specific protein level of hPGCLCs generated via 0.35% MC method and U96 method.

(A) Quantitative analysis of the expression of specific genes in EpCAM-/INTEGRINα6-high cells (day 4) via U96 method and 0.35% MC method, respectively. The error bars represent mean ± SD with three biological replicates (white, iMeLC; green, U96; red, MC). (B) Immunofluorescence analysis of OCT4, TFAP2C, BLIMP1 and SOX17 on day 4 embryoids from 0.35% MC method and U96 method. The nuclei were stained with Hoechst (left). Scale bars, 20 μm. (C) The proportion of Sox17 (+) cells at day 4 EBs via 0.35% MC method and U96 method (right); grey, U96; dark green, 0.35% MC; $^{**}P < 0.01$.

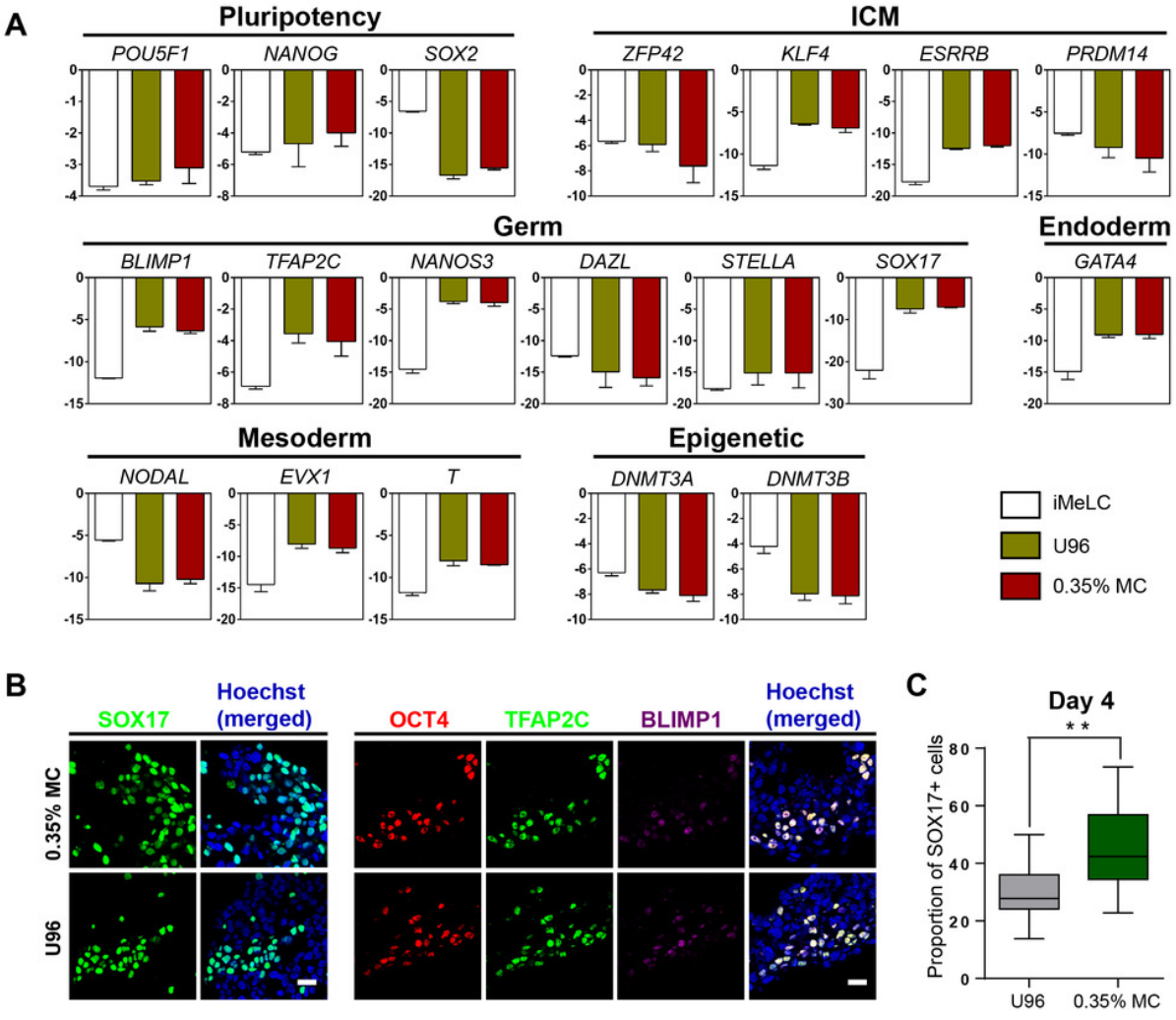
A
Pluripotency
POU5F1
NANOG
SOX2
ICM
ZFP42
KLF4
ESRRB
PRDM14
Germ
BLIMP1
TFAP2C
NANOS3
DAZL
STELLA
SOX17
Endoderm
GATA4
Mesoderm
NODAL
EVX1
T
Epigenetic
DNMT3A
DNMT3B
iMeLC
U96
0.35% MC
B
SOX17
Hoechst (merged)
OCT4
TFAP2C
BLIMP1
Hoechst (merged)
0.35% MC
U96
C
Day 4
* *
Proportion of SOX17+ cells
U96
0.35% MC

Figure 3

Epigenetic properties and cellular states of hPGCLCs generated via 0.35% MC method and U96 method.

(A) Immunostaining of H3K9me2 (top) and H3K27me3 (bottom) of EpCAM-/INTEGRINα6-high cells from U96 (left) or 0.35% MC (right) and the quantification of relative fluorescence intensity. ****$P < 0.0001$. Scale bars, 20 μm. (B) Immunostaining for 5hmC of EpCAM-/INTEGRINα6-high cells from U96 (top) and 0.35% MC (bottom) and the quantification of relative fluorescence. ***$P < 0.001$, ****$P < 0.0001$. Scale bar, 20 μm. (C) FACS analysis of cells in the P1 gates (living cells) of day 4 EBs from U96 and 0.35% MC (left). The statistics for ratios of P1 gates of day 4 and day 6 EBs from U96 and 0.35% MC were shown (right). At least four independent experiments were performed. (D) FACS analysis of the cell cycle states of day 4 EBs from U96 and MC. (E) FACS analysis of the apoptosis of day 4 EBs from U96 and 0.35% MC using 7AAD and Annexin V. (F) Immunostaining of TFAP2C and Ki67 of day 4 EBs from U96 or 0.35% MC (left) and the quantification of relative fluorescence intensity (right). Scale bar, 20 μm.

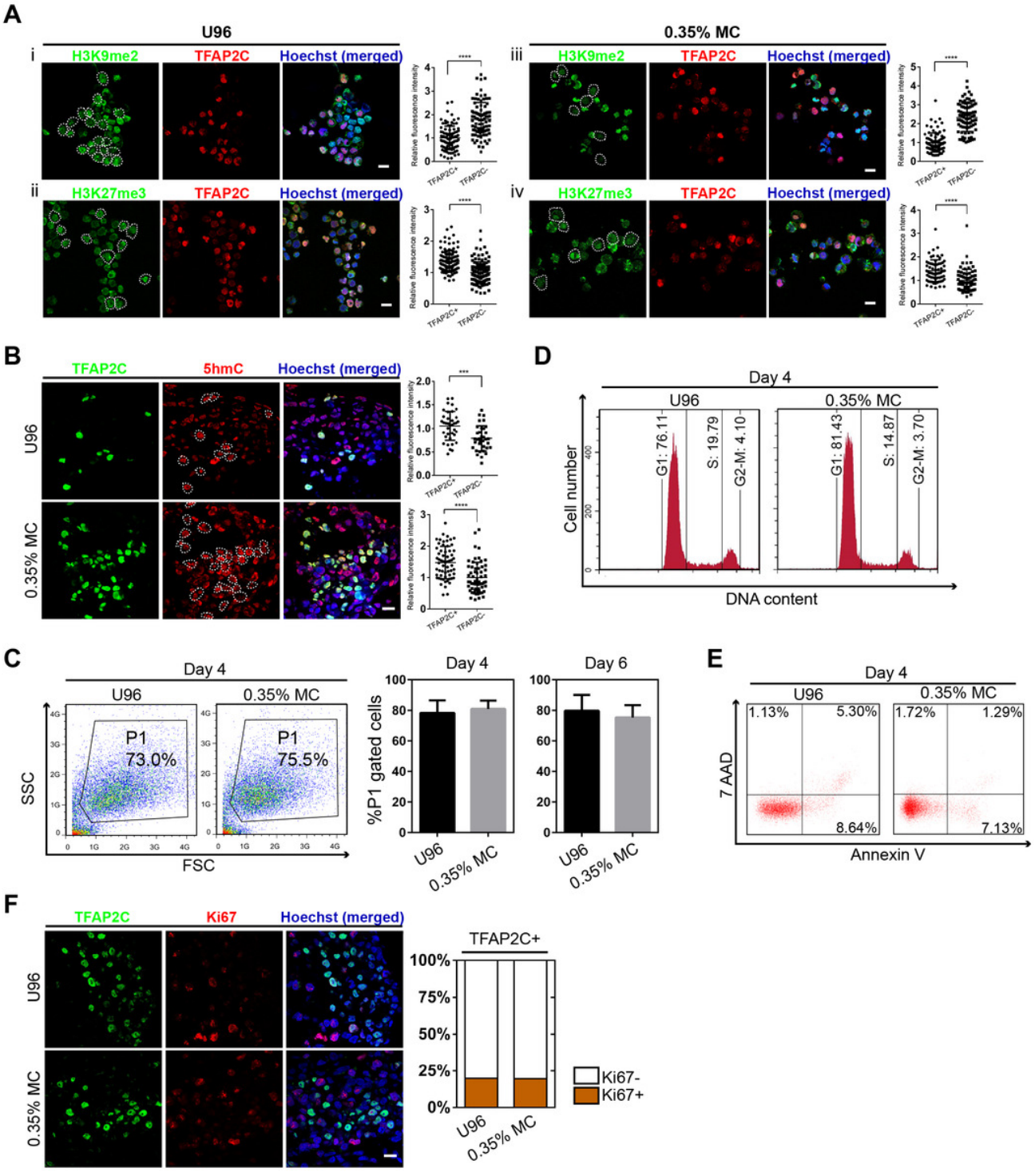
A
U96
0.35% MC
i
H3K9me2
TFAP2C
Hoechst (merged)
ii
H3K27me3
iii
iv
Relative fluorescence intensity
TFAP2C+
TFAP2C-
B
5hmC
U96
0.35% MC
C
Day 4
Day 6
P1
73.0%
75.5%
SSC
FSC
%P1 gated cells
D
Cell number
DNA content
G1: 76.11
S: 19.79
G2-M: 4.10
G1: 81.43
S: 14.87
G2-M: 3.70
E
7 AAD
Annexin V
1.13%
5.30%
8.64%
1.72%
1.29%
7.13%
F
Ki67
Ki67-
Ki67+

Figure 4

High induction efficiency of hPGCLCs from hiPSCs via MC method.

(A) Flow chart of the iPSC induction from the testicular cells of one OA patient and hPGCLC differentiation from hiPSCs via U96 method or MC method, respectively. (B) FACS analysis of the expression of EpCAM and INTEGRINα6 during the hPGCLC induction (at day 4) via U96 method and 0.35% MC method, respectively. (C) Quantitative gene expression analyses of specific genes in the iMeLCs and EpCAM-/INTEGRINα6-high cells generated via U96 method and 0.35% MC method, respectively. The error bars represent mean ± SD with at least two biological replicates. (D) Immunostaining of OCT4, TFAP2C and SOX17 on day 4 EBs from 0.35% MC (top) and U96 (bottom). The nuclei were stained with Hoechst. Scale Bars, 20 μm. (E, F) Immunostaining of H3K9me2, H3K27me3 (E) and 5hmC (F) in the EpCAM-/INTEGRINα6-high cells generated via U96 method or 0.35% MC method, respectively and the quantification of relative fluorescence intensity. ***$P < 0.001$, ****$P < 0.0001$. Scale bars, 20 μm.

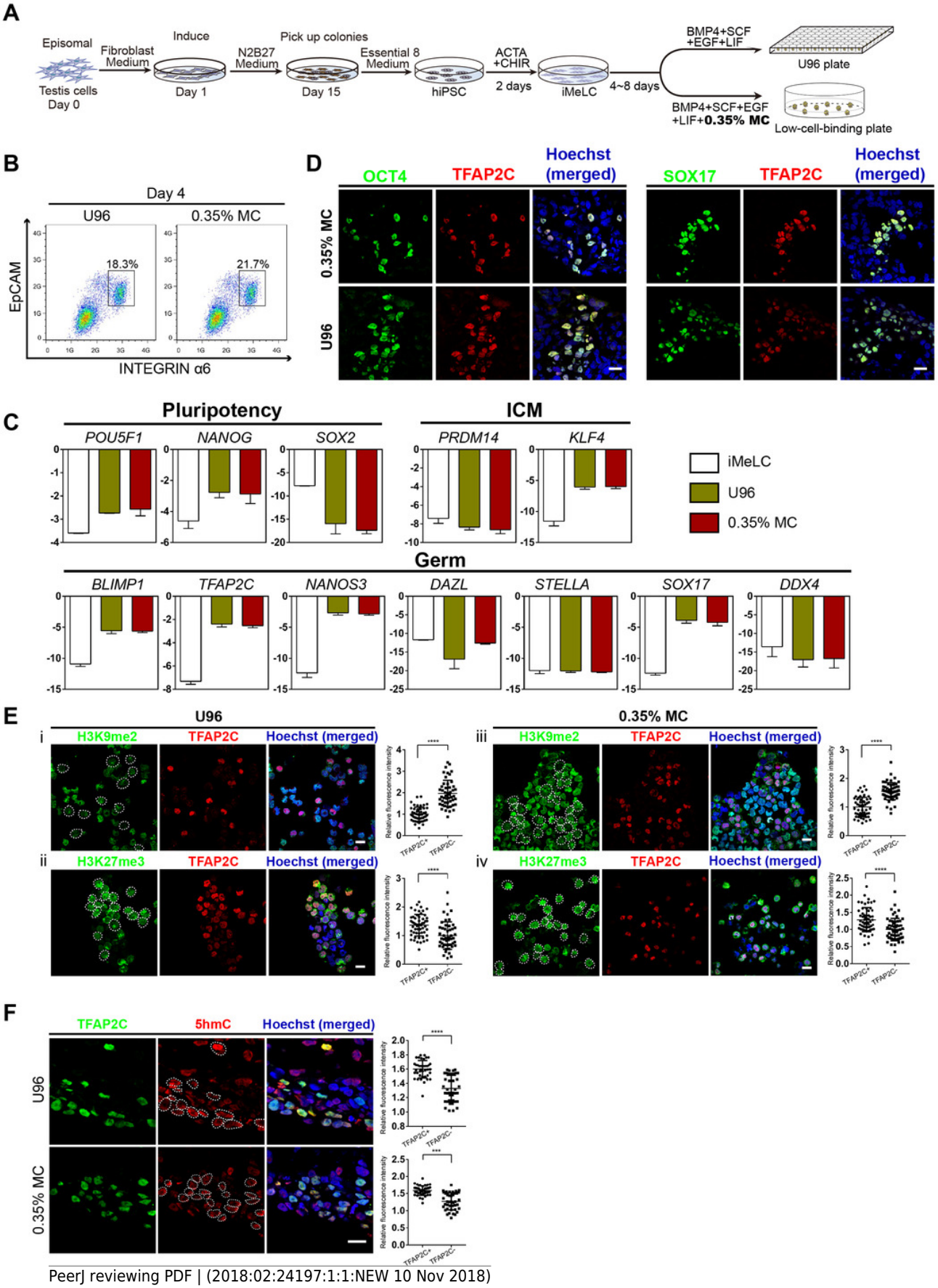
A
Episomal
Testis cells
Day 0
Fibroblast Medium
Induce
Day 1
N2B27 Medium
Pick up colonies
Day 15
Essential 8 Medium
hiPSC
ACTA +CHIR
2 days
iMeLC
4~8 days
BMP4+SCF +EGF+LIF
U96 plate
BMP4+SCF+EGF +LIF+0.35% MC
Low-cell-binding plate
B
Day 4
U96
0.35% MC
18.3%
21.7%
EpCAM
INTEGRIN α6
D
OCT4
TFAP2C
Hoechst (merged)
SOX17
TFAP2C
Hoechst (merged)
0.35% MC
U96
C
Pluripotency
POU5F1
NANOG
SOX2
ICM
PRDM14
KLF4
iMeLC
U96
0.35% MC
Germ
BLIMP1
TFAP2C
NANOS3
DAZL
STELLA
SOX17
DDX4
E
U96
0.35% MC
i
H3K9me2
TFAP2C
Hoechst (merged)
ii
H3K27me3
TFAP2C
Hoechst (merged)
iii
H3K9me2
TFAP2C
Hoechst (merged)
iv
H3K27me3
TFAP2C
Hoechst (merged)
Relative fluorescence intensity
TFAP2C+
TFAP2C-
F
TFAP2C
5hmC
Hoechst (merged)
U96
0.35% MC
Relative fluorescence intensity

Table 1(on next page)

The Yields of hPGCLCs of day 4 EBs via U96 method and 3D MC method.

Table 1:

The Yields of hPGCLCs of day 4 EBs via U96 method and 3D MC method.

Methods	Num. of seeding cells of one U96 plate or one well of 6-well plates from MC group	Num. of hPGCLCs of one U96 plate or one well of 6-well plate from MC group	Num. of hPGCLCs for each experiment (3x U96 plates or 3x 6-well plates from MC group)	The ratio of hPGCLCs yield (MC group vs U96 group for each experiment)
U96	$3.5x10^5$	$\sim5x10^4$	$15x10^4$	~9.6
MC	$5.0x10^5$	$\sim8x10^4$	$144x10^4$	